

In Situ Ligand-Transformation-Involved Synthesis of Inorganic–Organic Hybrid Polyoxovanadates as Efficient Heterogeneous Catalysts for the Selective Oxidation of Sulfides

Xiang Wang,* Tong Zhang, Yunhui Li, Jiafeng Lin, Huan Li, and Xiu-Li Wang*

Cite This: <https://dx.doi.org/10.1021/acs.inorgchem.0c02798>

Read Online

ACCESS |



Metrics & More

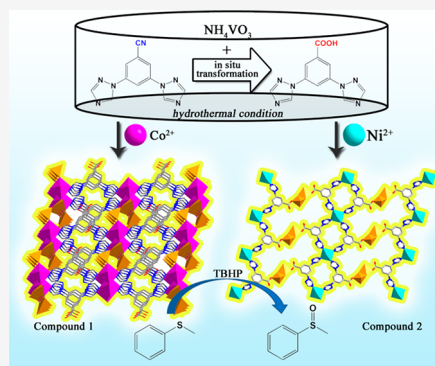


Article Recommendations



Supporting Information

ABSTRACT: By intentionally involving in situ ligand transformation in the reaction system, two inorganic–organic hybrid polyoxovanadates (POVs), [Co(HDTBA)V₂O₆] (1) and [Ni(H₂O)₂(DTBA)₂V₂O₄(OH)₂]·4H₂O (2), have been synthesized by using a hydrothermal method, where the 3,5-di[1,2,4]triazol-1-ylbenzoic acid (HDTBA) ligand originated from in situ hydrolysis of 3,5-di[1,2,4]triazol-1-ylbenzonitrile in the self-assembly process. The inorganic layers [Co₂(V₄O₁₂)_n] containing [V₄O₁₂]^{4−} circle clusters were linked by HDTBA ligands to yield a 3D framework structure of compound 1. There existed a kind of binuclear [(DTBA)₂V₂O₄(OH)₂]^{2−} vanadium cluster grafted directly by two DTBA ligands through the sharing of carboxyl oxygen atoms in compound 2, further extended into a 2D layer by nickel centers. The investigations on the catalytic properties indicated that compounds 1 and 2 as heterogeneous catalysts, especially 2, owned satisfying catalytic performances for catalyzing the selective oxidation of sulfides to sulfoxides in the presence of *tert*-butyl hydroperoxide as an oxidant, accompanied by excellent conversion of 100% and selectivity of above 99%, providing a promising way for developing inorganic–organic hybrid POVs as effective heterogeneous catalysts for catalyzing the selective oxidation of sulfides.



INTRODUCTION

More and more attention has been paid to the preparation of inorganic–organic hybrids based on polyoxometalates (POMs) because of their potential applications in the field of catalysis,^{1–3} batteries,⁴ supercapacitors,⁵ and photochemistry and electrochemistry.^{6–8} As a remarkable branch of POMs, polyoxovanadate (POV)-based inorganic–organic hybrids are of considerable interest not only because of their remarkable properties such as magnetism⁹ and catalysis and fluorescence^{10,11} but also because of their diverse architectures.^{12,13} In the synthesis of POV-based hybrids with various structures and outstanding properties, on the one hand, the selection and design of organic ligands is very important. A universal pathway is to introduce the organic ligands into the reaction system to construct POV-based hybrids. Up to now, a large number of presynthesized organic ligands have been involved in the structures of POV-based hybrids, including not only bidentate nitrogen-donor ligands such as 1,2-di(4-pyridyl)-ethylene and 1,4-bis(imidazol-1-yl)butane as well as multi-dentate such as 2,4,6-tri(4-pyridyl)-1,3,5-triazine and so on, which have been summarized well in the review organized by Arriortua in 2014,¹⁴ but also many carboxylic acid ligands,^{15–17} with the addition of those combining the nitrogen-donor group and carboxylic acid.^{18,19} It should be pointed out that most organic ligands in these works are presynthesized and used directly, which prompts us to continue to design and develop

more presynthesized organic ligands for exploiting POV-based hybrids with various structures.

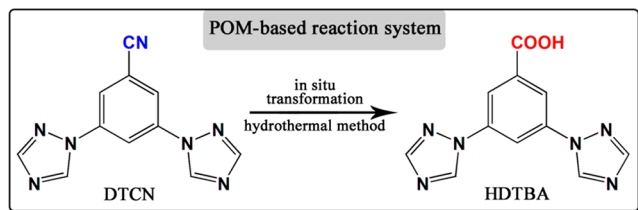
On the other hand, POV-based inorganic–organic hybrids have been mentioned as a kind of efficient heterogeneous catalyst for the oxidation of sulfide. For instance, not only can the use of organic ligands, including 1,4-bis(1*H*-imidazol-1-yl)benzene,²⁰ 1,10-phenanthroline,²¹ resorcin[4]arene,²² ethanediamine, 1,2-cyclohexanediamine, and 1,2-diaminopropane,²³ generate charming architectures based on POVs, but also these hybrids exhibited high efficiency and selectivity in the oxidation of sulfides, suggesting that the continuous design and synthesis of POV-based hybrids may be promising to develop efficient catalysts used in the selective sulfoxidation of sulfides.

In our group's previous works, deliberately involving in situ ligand transformation in the reaction system has been considered to be a feasible pathway for the synthesis of POM-based hybrids,^{24–26} where not only were the N-bidentate ligands containing nitrile groups [3,5-di(1*H*-

Received: September 22, 2020

imidazol-1-yl)benzonitrile (DTCN), 3,5-di[1,2,4]triazol-1-yl-benzonitrile (DTCN), and 3,5-di(benzimidazolyl-1-yl)-benzonitrile] hydrolyzed in situ into new N-bidentate ligands containing carboxylic acid in the final structures (Scheme 1),

Scheme 1. Representative In Situ Ligand Transformation



but also the generated ligands can participate in the formation of POM-based hybrids, together with various structural features. Inspired by the above results, in situ ligand transformation was intentionally introduced into the reaction system based on POVs that may be a hopeful pathway for the preparation of POV-based inorganic–organic hybrids with innovative architectures and catalytic properties.

Here, when DTCN was selected as the initial ligand, two POV-based hybrids with the formulas of $[\text{Co}(\text{HDTBA})\text{V}_2\text{O}_6]$ (**1**) and $[\text{Ni}(\text{H}_2\text{O})(\text{DTBA})_2\text{V}_2\text{O}_4(\text{OH})_2] \cdot 4\text{H}_2\text{O}$ (**2**) were isolated by changing metal ions under hydrothermal conditions, in which 3,5-di[1,2,4]triazol-1-ylbenzoic acid (HDTBA) involved in the formation of hybrid structures was derived from in situ hydrolysis of DTCN. Among them, compound **1** was a 3D framework built from $[\text{Co}_2(\text{V}_4\text{O}_{12})]_n$ inorganic layers consisting of $[\text{V}_4\text{O}_{12}]^{4-}$ circle clusters and HDTBA ligands as linkers, and compound **2** possessed a 2D layer structure composed of POV building units $[(\text{DTBA})_2\text{V}_2\text{O}_4(\text{OH})_2]^{2-}$ modified directly by DTBA ligands. Further, the studies on the catalytic performance using **1** and **2** as heterogeneous catalysts revealed that all compounds have high activity and selectivity toward the oxidation of sulfide to sulfoxide with *tert*-butyl hydroperoxide (TBHP) as the oxidant. The magnetic behavior of compound **1** was also investigated here.

EXPERIMENTAL SECTION

Materials and Methods. Available reagents and solvents used in this paper were purchased from commercial sources and used without further purification. The DTCN ligand was prepared in accordance with the method reported in the literature.²⁷

Physical Measurements. The chemical composition of all complexes was calculated from elemental analyses (carbon, hydrogen, and nitrogen) on a PerkinElmer 2400C elemental analyzer. Fourier transform infrared (FT-IR) spectra were recorded on a Scimitar 2000 near-FT-IR spectrometer with KBr pellets. Powder X-ray diffraction (PXRD) data were collected on a Rigaku Ultima IV diffractometer at room temperature. The catalytic reaction was analyzed by using a Shimadzu Techcomp GC-7900 gas chromatograph with an flame ionization detector equipped with a TM-5 Sil capillary column, where naphthalene was selected as an internal standard substrate. Gas chromatography (GC)–mass spectrometry (MS) spectra were recorded on an Agilent 7890A-5975C spectrometer. The temperature-dependent magnetic susceptibility data were collected on a SQUID magnetometer in the temperature range of 2–300 K under a 1 kOe field.

Synthesis of $[\text{Co}(\text{HDTBA})\text{V}_2\text{O}_6]$ (1**).** A mixture of NH_4VO_3 (0.06 g, 0.5 mmol), $\text{CoCl}_2 \cdot 6\text{H}_2\text{O}$ (0.06 g, 0.25 mmol), DTCN (0.06 g, 0.25 mmol), and 10 mL of deionized water was stirred at room temperature for 1 h, and then the pH value was adjusted to about

4.0 using a 1.0 M HCl solution, which was further placed in a 25 mL Teflon-lined autoclave and heated at 160 °C for 4 days. Red block-shaped crystals were isolated with a yield of 34% based on NH_4VO_3 . Anal. Calcd for $\text{C}_{11}\text{H}_7\text{CoN}_6\text{O}_8\text{V}_2$ (512.04): C, 25.80; H, 1.28; N, 16.41. Found: C, 25.69; H, 1.42; N, 16.32. IR (solid KBr pellets, cm^{-1}): 1740 (s), 1688 (s), 1610 (s), 1521 (s), 944 (s), 903 (s), 848 (s), 794 (s).

Synthesis of $[\text{Ni}(\text{H}_2\text{O})(\text{DTBA})_2\text{V}_2\text{O}_4(\text{OH})_2] \cdot 4\text{H}_2\text{O}$ (2**).** The synthesis process of complex **2** was similar to that of **1**, except that $\text{CoCl}_2 \cdot 6\text{H}_2\text{O}$ was replaced with $\text{NiCl}_2 \cdot 6\text{H}_2\text{O}$ (0.06 g, 0.25 mmol) or DTCN (0.12 g, 0.5 mmol). Light-green block-shaped crystals were obtained with a yield of 34% based on NH_4VO_3 . Anal. Calcd for $\text{C}_{22}\text{H}_{24}\text{N}_{12}\text{NiO}_{16}\text{V}_2$ (873.07): C, 30.27; H, 2.77; N, 19.25. Found: C, 30.17; H, 2.91; N, 19.16. IR (solid KBr pellet, cm^{-1}): 3431 (w), 1600 (s), 1538 (s), 1460 (s), 928 (s), 874 (s), 782 (s).

General Procedure for the Catalytic Oxidation of Sulfides. Sulfide (0.5 mmol), TBHP (0.75 mmol), catalyst (3 μmol , 0.6 mol %), and 2 mL of methanol were placed in a 5 mL round-bottom flask. The catalytic reaction was operated at 50 °C for 15 min and monitored by GC at various time intervals. The products were analyzed by GC–MS.

X-ray Crystallographic Study. The data crystallographic data of complexes **1** and **2** were acquired on a Bruker SMART APEX II with Mo $K\alpha$ ($\lambda = 0.71073$ Å) at 298 K. These structures were solved by direct methods employing the *SHELXT 2014* program packages.^{28,29} Refinement of the structure was finished by full-matrix least-squares methods based on F^2 . The hydrogen atoms belonging to coordination and lattice water molecules were not located in the structures but embodied in the structure factor calculations. The detailed crystallographic data for complexes **1** and **2** are summarized in Table 1. Table S1 involves the selected bond lengths and angles.

Table 1. Crystal Data for Compounds **1** and **2**

	1	2
formula	$\text{C}_{11}\text{H}_7\text{CoN}_6\text{O}_8\text{V}_2$	$\text{C}_{22}\text{H}_{24}\text{N}_{12}\text{NiO}_{16}\text{V}_2$
fw	512.04	873.07
temperature/K	293(2)	293(2)
cryst syst	triclinic	triclinic
space group	$P\bar{1}$	$P\bar{1}$
<i>a</i> /Å	6.8675(8)	7.6969(7)
<i>b</i> /Å	9.3105(11)	10.5154(9)
<i>c</i> /Å	13.2286(16)	10.6644(9)
α /deg	101.571(2)	101.148(2)
β /deg	93.950(2)	101.397(2)
γ /deg	109.753(2)	104.148(2)
<i>V</i> /Å ³	771.27(16)	793.49(12)
<i>Z</i>	2	1
<i>D_c</i> /g·cm ^{−3}	2.205	1.806
μ /mm ^{−1}	2.313	1.259
<i>F</i> (000)	504	432
final R_1^a , wR_2^b [<i>I</i> > 2 σ (<i>I</i>)]	0.0371, 0.0879	0.0363, 0.0918
final R_1^a , wR_2^b (all data)	0.0501, 0.0941	0.0505, 0.1002
GOF of F^2	1.024	1.025

$$^a R_1 = \sum \|F_o\| - |F_c| / \sum \|F_o\|. \quad ^b wR_2 = [\sum w(F_o^2 - F_c^2)^2 / \sum w(F_o^2)^2]^{1/2}.$$

RESULTS AND DISCUSSION

Synthesis. The feasibility of intentionally using in situ ligand transformation to construct POM-based hybrids has been confirmed in our previous works, where the cyano group can be easily hydrolyzed in situ to a carboxylate group under hydrothermal conditions, and a few of inorganic–organic hybrids based on polymolybdates/polytungstates, including $[\text{PMo}_{12}\text{O}_{40}]^{3-}$, $[\text{SiW}_{12}\text{O}_{40}]^{4-}$, $[\text{P}_2\text{W}_{18}\text{O}_{62}]^{6-}$, and $[\text{Mo}_8\text{O}_{26}]^{4-}$, have been isolated. On the basis of the idea of developing more

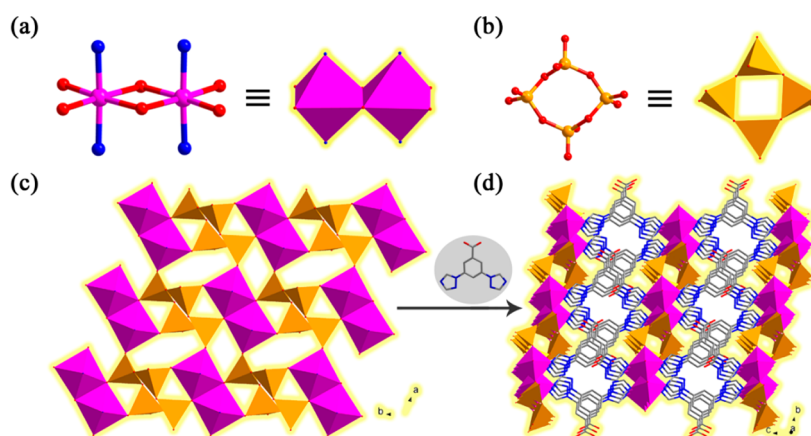


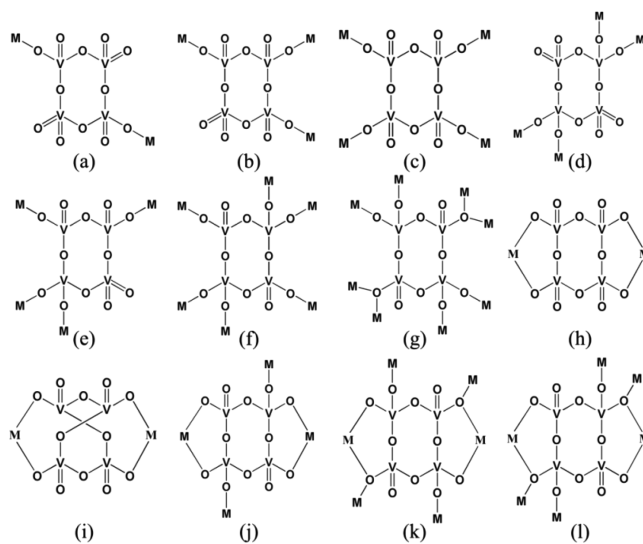
Figure 1. (a) View of the binuclear cobalt unit. (b) $[\text{V}_4\text{O}_{12}]^{4-}$ circular cluster constructed from two $\text{V}_2\text{O}_6^{2-}$ polyoxoanions. (c) 2D layer structure built from $\text{V}_2\text{O}_6^{2-}$ polyoxoanions and binuclear cobalt units. (d) 3D framework based on the POV of complex 1.

synthesis approaches for preparing POV-based hybrids, in situ ligand transformation was deliberately introduced into the reaction system to synthesize inorganic–organic hybrids based on the POVs here. As expected, the common features were that the DTCN ligand was hydrolyzed in situ to the HDTBA ligand and two POV-based hybrids with different architectures were isolated by tuning the metal ion and reaction conditions. When the Co^{2+} ion was chosen together with the molar ratio of 2:1:1 for $\text{Co}^{2+}/\text{NH}_4\text{VO}_3/\text{DTCN}$, the satisfactory red crystals of **1** were collected by controlling the pH values of 4.0–4.5. However, the cobalt vanadate mentioned by Ma's group can be generated at pH values above 4.5³⁰ and only an amorphous solid for pH values of less than 4.0, while crystals of **2** were not obtained under the same conditions as those of **1**. When the molar ratio of $\text{Ni}^{2+}/\text{NH}_4\text{VO}_3/\text{DTCN}$ was adjusted to 1:1:1, light-green crystals of **2** were obtained, but no crystals appeared under such a ratio for the Co^{2+} ion. In other words, the pH and ratio of raw materials exhibited important effects on the formation of crystalline **1** and **2**.

Crystal Structure of 1. Compound **1** consists of one cobalt(II) atom, one HDTBA ligand, and one $[\text{V}_2\text{O}_6]^{2-}$ polyoxoanion. Bond-valence-sum calculations show that the cobalt and vanadium atoms are in the II+ and V+ oxidation states.³¹ The octahedral configuration of the Co^{2+} ion is defined by four oxygen atoms in the equatorial position and two nitrogen atoms from the HDTBA ligand in the apical position. Two octahedral Co^{2+} ions are aggregated through an edge-sharing mode to establish a binuclear cobalt unit (Figure 1a). Each of the crystallographically independent vanadium centers in a $[\text{V}_2\text{O}_6]^{2-}$ polyoxoanion surrounding four oxygen atoms possesses VO_4 tetrahedral coordination geometry. Two sets of $[\text{V}_2\text{O}_6]^{2-}$ polyoxoanions are linked by corner-sharing oxygen atoms to result in a $[\text{V}_4\text{O}_{12}]^{4-}$ circular cluster (Figure 1b). These $[\text{V}_4\text{O}_{12}]^{4-}$ clusters are connected by binuclear cobalt units to give rise to a 2D Co–O–V layer structure (Figure 1c), where the remaining terminal oxygen atoms belonging to the V1 center occupy the terminal and edge-sharing oxygen atoms of adjacent binuclear cobalt units, and only one terminal oxygen atom from the V2 center occupies the terminal oxygen atom of the binuclear cobalt units. Finally, the HDTBA ligands as bidentate linkers utilize two nitrogen atoms of the triazolyl group to coordinate with cobalt atoms from neighboring Co–O–V layers, yielding a 3D framework based on the POV of complex **1** (Figure 1d).

In **1**, one of the structural features is that the intentional in situ transformation of DTCN to the HDTBA ligand has been involved in constructing the POV-based hybrids as we expected. The other one represents a new mode of $[\text{V}_4\text{O}_{12}]^{4-}$ circular cluster coordination to metal ions. The $[\text{V}_4\text{O}_{12}]^{4-}$ clusters accompanied by various coordination modes with metal ions has generally been reported so far, which is summarized in Scheme 2. The $[\text{V}_4\text{O}_{12}]^{4-}$ cluster can

Scheme 2. Diverse Linking Modes of the $[\text{V}_4\text{O}_{12}]^{4-}$ Cluster



display polydentate coordination modes, where the terminal oxygen atom of the $[\text{V}_4\text{O}_{12}]^{4-}$ cluster is coordinated with the metal center in either a one-to-one manner (types a–f) or an occasional one-to-many manner (type g). Some mentioned types have been expounded by Spodine and co-workers.³² The other common bischelating modes, along with polydentate coordination pattern mode, were also involved in the reported cases of $[\{\text{Cd}(\text{phen})_2\}_2\text{V}_4\text{O}_{12}] \cdot 5\text{H}_2\text{O}$ (type h),³³ $[\{\text{Zn}(\text{bipy})_2\}_2\text{V}_4\text{O}_{12}]$,³⁴ $[\{\text{Co}_2(\text{H}_2\text{O})_2(\text{Bpe})_2\}(\text{V}_4\text{O}_{12})] \cdot 4\text{H}_2\text{O} \cdot \text{Bpe}$ (type j),³⁵ and $[\text{Cu}_3(\text{triazolate})_2\text{V}_4\text{O}_{12}]$ (type k).³⁶ In this work, compound **1** shows a new type l mode, including two chelate and four monodentate metal centers. The numbers of metal centers around the $[\text{V}_4\text{O}_{12}]^{4-}$ cluster are the same as those of types f and k, but the difference from type k is the

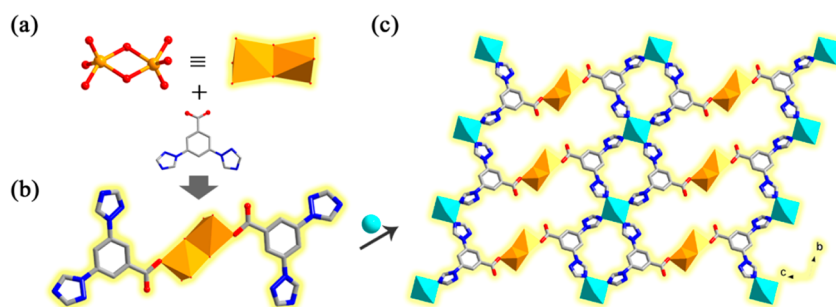


Figure 2. (a) View of the binuclear vanadium cluster $[\text{V}_2\text{O}_6(\text{OH})_2]^{4-}$. (b) Binuclear $[(\text{DTBA})_2\text{V}_2\text{O}_4(\text{OH})_2]^{2-}$ building unit modified by the DTBA ligands. (c) 2D layer structure based on the POV of complex 2.

position of the oxygen atoms involved in the monodentate coordination mode.

Crystal Structure of Compound 2. In 2, the crystallographically independent vanadium atom in the V+ oxidation state is five-coordinated,³¹ completed by three oxygen atoms and two hydroxy groups. A pair of vanadium atoms are each gathered through sharing two μ_2 -OH groups, generating a binuclear vanadium cluster $[\text{V}_2\text{O}_6(\text{OH})_2]^{4-}$ (Figure 2a). Interestingly, the binuclear vanadium cluster $[\text{V}_2\text{O}_6(\text{OH})_2]^{4-}$ is further decorated by two DTBA ligands, where two terminal oxygen atoms of the vanadium cluster $[\text{V}_2\text{O}_6(\text{OH})_2]^{4-}$ are shared by oxygen atoms of the carboxyl group (Figure 2b), forming a $[(\text{DTBA})_2\text{V}_2\text{O}_4(\text{OH})_2]^{2-}$ building unit. In fact, a series of isopolymolybdate-based hybrids modified by the carboxyl group stemming from in situ ligand transformation of the cyano group have been obtained in our previous works, where DICN and DTCN were chosen as the initial ligands. However, the POVs modified by the carboxyl group originating from in situ ligand transformation of the cyano group are scarce. These findings allow one to conclude that in situ POMs could usually be easily grafted by in situ ligands,^{25,26} but it rarely occurs in the reaction system based on classical POMs, such as Keggin POMs $[\text{PMo}_{12}\text{O}_{40}]^{3-}$ and $[\text{SiW}_{12}\text{O}_{40}]^{4-}$ and the Wells–Dawson POM $[\text{P}_2\text{W}_{18}\text{O}_{62}]^{6-}$,²⁴ which suggests a potential approach for preparing the POM-based complexes modified by in situ ligand transformation. Further, the $[(\text{DTBA})_2\text{V}_2\text{O}_4(\text{OH})_2]^{2-}$ building units as tetradentate linkages relying on four nitrogen atoms of the imidazolyl group from two DTBA ligands are linked by nickel centers to give a 2D layer structure of 2 (Figure 2c), and the coordination of two water molecules compensates for the octahedral configuration of each nickel center.

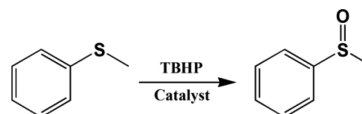
PXRD, FT-IR Spectra, and Thermogravimetric (TG) Analyses. PXRD experiments of two compounds were carried out to confirm the phase purities, as shown in Figure S1. The experimental diffraction peaks of compounds 1 and 2 are in accordance with the patterns simulated by single-crystal analysis of 1 and 2, revealing that the phase purities of two compounds are satisfactory. The FT-IR spectra of compounds 1 and 2 are present in Figure S2. The characteristic bands in the region of 950–540 cm^{-1} should be derived from the absorption peaks of $\text{V}=\text{O}$ and $\text{V}-\text{O}-\text{V}$.³⁷ The bands in the region of 1743–1400 cm^{-1} should be ascribed to the characteristic peaks of the DTBA ligand.²⁵ TG analyses of 1 and 2 were also provided to verify the composition of the structure. Figure S3 embodies one step of the weight loss process for 1, about 50.84% (calcd 49.8%) ascribed to the decomposition of organic ligands, two steps of the weight loss process for 2, about 13.1% (calcd 12.4%) and 57.6% (calcd

58.4%) belonging to decomposition of the water molecules and organic ligands, respectively.

Magnetic Properties. The magnetic susceptibility depending on the temperature from 2 to 300 K of compound 1 was investigated with a 1 kOe field, and the curves of χ_M versus T and χ_M^{-1} versus T are demonstrated in Figure S4. The $\chi_M T$ value of 4.22 $\text{cm}^3 \text{K mol}^{-1}$ at 300 K is much larger than the expected $\chi_M T$ value of two isolated cobalt(II) ions (3.875 $\text{cm}^3 \text{K mol}^{-1}$ with $g = 2$ and $S = 3/2$), embodying the fact that the orbital contribution derived from distorted octahedral cobalt(II) centers is important.^{38,39} The plot of $\chi_M T$ versus T displays a continuous decrease with a change in the temperature from 300 to 2 K, and the $\chi_M T$ value reaches 2.13 emu K mol^{-1} at 2 K. The magnetic susceptibility in the range of 2–300 K of compound 1 obeys the Curie–Weiss equation $[\chi_M = C/(T - \theta)]$ with Weiss constants $\theta = -9.72 \text{ K}$ and $C = 4.41 \text{ cm}^3 \text{K mol}^{-1}$, suggesting that an antiferromagnetic coupling stemmed from the binuclear cobalt(II) unit in 1.

Catalytic Oxidation of Sulfides. Selective oxidation of sulfides to sulfone and sulfoxide has drawn extensive attention because of their widespread application in the preparation of biological molecules,⁴⁰ as auxiliaries in asymmetric and chiral synthesis,⁴¹ where the hybrids based on POVs represented kinds of very popular candidates as catalysts for the selective oxidation of sulfides.⁴² Herein, the catalytic activities of compounds 1 and 2 for oxidizing sulfide to sulfoxide were investigated in detail. A typical modal reaction with methyl phenyl sulfide (MPS) as the substrate was established to evaluate the selective catalytic abilities of compounds 1 and 2 using TBHP as the oxidant (Scheme 3).

Scheme 3. Selective Oxidation of MPS to Sulfoxide Catalyzed by Compounds 1 and 2



The heterogeneous catalytic efficiencies of 1 and 2 for the selective oxidation of MPS to sulfoxide were assessed by changes in the reaction conditions, including temperature, dosage of the catalyst, oxidants, and reaction time, and the catalytic results were analyzed by GC, as shown in Table 2. The catalytic reactions with TBHP as the oxidant and 2 as the catalyst were first carried out at room temperature and 50 and 60 °C for 15 min in methanol, and the dosages of the substrate, catalyst, and TBHP were 0.5 mmol, 3 μmol , and 0.5 mmol (entry 3). The catalytic results revealed that the

Table 2. Conversion and Selectivity of the Oxidation of MPS to Sulfoxide Analyzed by 2 with TBHP as the Oxidant in Methanol^a

entry	catalyst (μmol)	TBHP (mmol)	time (min)	temp ($^{\circ}\text{C}$)	convn (%) ^b	selectivity (%) ^c
1	3	0.5	15	rt	<10	
2	3	0.5	15	50	83	98
3	3	0.5	15	60	98	84
4	3	0.75	15	50	100	99
5	3 ^d	0.75	15	50	98	98
6	4	0.75	15	50	92	99
7	3	1	15	50	98	84
8	3	0.75	10	50	88	99
9	3	0.75	20	50	100 ^a , 100 ^d	89 ^a , 94 ^d
10	3	none	15	50	<1	
11	none	0.75	15	50	<20	
12	3 ^e	0.75	15	50	75	98
13	3 ^f	0.75	15	50	79	98
14	3 ^g	0.75	15	50	82	99

^aReaction conditions: substrate, 0.5 mmol; methanol, 2 mL; compound 2, 3 μmol (0.6 mol %). ^bThe conversion and selectivity to sulfoxides were confirmed by GC. ^cSelectivity (%) = sulfoxide (mol)/sulfone (mol) \times 100. ^dCompound 1. ^eEthanol (2 mL). ^fTrichloromethane (2 mL). ^gAcetonitrile (2 mL).

temperature of 60 $^{\circ}\text{C}$ led to a gratifying conversion of 98% but only 84% for the selectivity of MPS to sulfoxide. The selectivity was further promoted to 98% along with a reduction in the reaction temperature to 50 $^{\circ}\text{C}$; nevertheless, the conversion is only 83% (entry 2). Subsequently, when the dosage of TBHP was increased to 0.75 mmol, the conversion and selectivity of 100% and 99% were gratifying (entry 4), until the dosage of 1 mmol resulted in a declining selectivity of 84% (entry 7), which is superior to the previously reported POV-based inorganic–organic hybrids, such as $[\text{Cu}(\text{mIM})_4]\text{V}_2\text{O}_7$,⁴³ $[\text{Co}_2\text{-I}_{0.5}\text{V}_{4.5}\text{O}_{12}]\cdot 3\text{DMF}\cdot 5\text{H}_2\text{O}$,²² $[(\text{C}_2\text{N}_2\text{H}_8)_4(\text{CH}_3\text{O})_4\text{V}^{\text{IV}}_4\text{V}^{\text{V}}_4\text{O}_{16}]\cdot 4\text{CH}_3\text{OH}$,⁴⁴ $\text{K}_6\text{H}[\text{V}^{\text{V}}_{17}\text{V}^{\text{IV}}_{12}(\text{OH})_4\text{O}_{60}(\text{OOC}(\text{CH}_2)_4\text{COO})_8]\cdot n\text{H}_2\text{O}$,¹⁵ and so on but comparable to the aforementioned example (en) $[\text{Cu}_3(\text{ptz})_4(\text{H}_2\text{O})_4][\text{Co}_2\text{Mo}_{10}\text{H}_4\text{O}_{38}]\cdot 24\text{H}_2\text{O}$.⁴⁵ Following continual attempts to enhance the selectivity in the oxidation of MPS to sulfoxide by tuning the above factors, including the dosage of the catalyst (entry 6), reaction time (entries 8 and 9), solvent types (ethanol, trichloromethane, and acetonitrile; entries 12–14), no more satisfying results were obtained. Obviously, the optimum reaction time and temperature for oxidizing MPS to sulfoxide with 2 as the catalyst are 15 min and 50 $^{\circ}\text{C}$ in methanol, and the appropriate mole ratio of $n_{\text{substrate}}:n_{\text{oxidant}}:n_{\text{catalyst}}$ was 1:1.5:0.6%. Besides, the catalytic performance of 1 for the oxidation of MPS to sulfoxide was also carried out under the above optimum condition. The good conversion and selectivity of 98% were obtained (entry 5), until 100% and 94% with increasing reaction time to 20 min (entry 9), which are lower than that using 2 as the catalyst, which may be caused by their different structures, namely, a 3D framework for 1 but a 2D layer network for 2, leading to the difference in exposed active sites.⁴³ The blank experiments without any analysts or oxidants under optimum conditions were performed, and the effective oxidation activity of MPS to sulfoxide was not observed. Although the oxidation reaction can also occur in the presence of the oxidant alone, the conversion of 20% is very low (entries 10 and 11). So, the excellent oxidation reaction with 1 and 2 as

catalysts suggested that the catalytic reaction may focus on organic–inorganic hybrid-based POVs.

The catalytic activities of the raw material NH_4VO_3 and corresponding complexes have been further studied to demonstrate whether 1 and 2 as the representatives of a combination of complexes and POVs has the advantage of catalyzing the oxidation of MPS to sulfoxide. As shown in Table 3, using NH_4VO_3 as the catalyst under optimum

Table 3. Conversion and Selectivity of MPS to Sulfoxide by Using Different Catalysts^a

catalyst	convn (%)	selectivity (%)
1	98	98
2	100	99
NH_4VO_3	65	86
$[\text{Co}(\text{H}_2\text{O})_2(\text{DTBA})_2]\cdot 3\text{H}_2\text{O}$	<1	
$[\text{Ni}(\text{H}_2\text{O})_2(\text{DTBA})_2]\cdot 3\text{H}_2\text{O}$	<13	

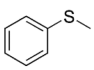
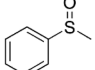
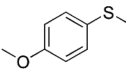
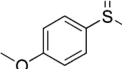
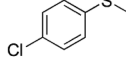
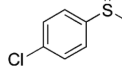
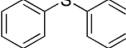
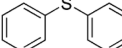
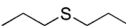
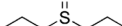
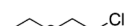
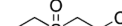
^aReaction conditions: MPS, 0.5 mmol; catalyst, 3 μmol (0.6 mol %); TBHP, 0.75 mmol; methanol, 2 mL; 50 $^{\circ}\text{C}$; 15 min.

conditions, a conversion of 65% and a selectivity of 86% were obtained. The conversions were less than 1% and 13% when complexes $[\text{Co}(\text{H}_2\text{O})_2(\text{DTBA})_2]\cdot 3\text{H}_2\text{O}$ and $[\text{Ni}(\text{H}_2\text{O})_2(\text{DTBA})_2]\cdot 3\text{H}_2\text{O}$ were selected as the catalysts (Scheme S1 and Figure S5). These results reveal that the combination of complexes and POVs can generate heterogeneous catalysts (1 and 2) with excellent conversion and selectivity for the oxidation of MPS to sulfoxide, which was in accordance with the reported findings of the cation and polyoxoanion parts enhancing the selectivity and conversion of substrates.^{43,46} The catalytic mechanism speculated that the POVs as catalytic active sites in the structures of complexes were attacked by an oxidant during the catalytic process to form metal peroxide intermediates, and the sulfide was then oxidized to sulfoxide by the intermediate of the metal peroxide.^{44,46,47}

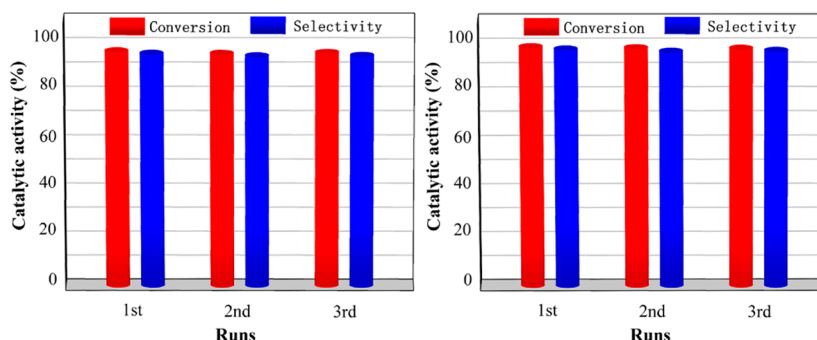
Considering the best catalytic property of 2, several sulfides with electron donor and acceptor groups, different steric effects of 4-methoxythioanisole, 4-chlorothioanisole, diphenyl sulfide, and alkyl thioethers such as dipropyl sulfide and 2-chloroethyl ethyl sulfide, were chosen as substrates to evaluate further sulfoxidation catalyzed by 2 under the optimum conditions. As shown in Table 4, the corresponding obtained products were analyzed by GC–MS (Figure S6). The introduction of the electron donor and acceptor groups to MPS results in a slight decrease of the catalytic oxidation conversion in comparison with that of MPS (Table 4, entries 1–3); especially, a larger steric resistance containing a substrate like diphenyl sulfide exhibits obvious decreases of the conversion and selectivity (Table 4, entry 4), similar to the reported results.^{21,48} Subsequently, the alkyl thioethers with less steric hindrance, such as dipropyl sulfide and 2-chloroethyl ethyl sulfide, were assigned as substrates; not only were satisfying conversion and selectivity values comparable to that of MPS, but also less time (10 min) and a low temperature (40 $^{\circ}\text{C}$) were required (Table 4, entries 5 and 6). That is to say, the steric hindrance of the substrate displays an important influence on the conversion of sulfide to sulfoxide.

The reutilization and stability are recognized as significant factors for excellent heterogeneous catalysts. The recycle sulfoxidation reactions of MPS to sulfoxide catalyzed by compounds 1 and 2 were first carried out under optimum

Table 4. Results of Selective Oxidation of Various Sulfides to Sulfoxides by Using **2** as the Catalyst^a

Entry	Substrate	Products	Conv. (%)	Sel. (%)
1			100	99
2			97	98
3			96	98
4 ^b			94	95
5 ^c			99	98.6
6 ^c			99	99

^aReaction conditions: substrate, 0.5 mmol; methanol, 2 mL; TBHP, 0.75 mmol; compound **2**, 3 μ mol (0.6 mol %); 50 °C; 15 min. ^b25 min. ^c40 °C, 10 min.

Figure 3. Recycling of compounds **1** (left) and **2** (right) as catalysts for the sulfoxidation of MPS.

conditions for assessing the recyclability of the catalysts. After the reaction finished, the catalysts filtered from the reaction mixture were washed using methanol and reused to catalyze the oxidation of MPS to sulfoxide, revealing that compounds **1** and **2** as the catalysts can be reused for at least three runs without obvious loss of catalytic performance (Figure 3). Moreover, the PXRD patterns of the recycled catalysts are consistent with that simulated by the crystal data (Figure S7), manifesting that the catalysts are stable after catalysis and recycling.

CONCLUSIONS

In a word, two inorganic–organic hybrid POVs have been assembled depending on the in situ ligand transformation of DTCN to HDTBA, which afforded not only a kind of $[V_4O_{12}]^{4-}$ circle cluster with a new coordination mode in the 3D structure of **1** but also yielded a binuclear $[(DTBA)_2V_2O_4(OH)_2]^{2-}$ vanadium cluster modified directly by DTBA ligands in the 2D layer of **2**. Magnetic investigations reveal that compound **1** exhibits an antiferromagnetic behavior. Furthermore, two compounds as heterogeneous catalysts, especially **2**, showed efficient catalysis for the selective oxidation of sulfides to sulfoxides with excellent recyclability and reusability. The above findings may provide a potential

strategy for preparing POV-based inorganic–organic hybrids and exploiting effective heterogeneous catalysts toward the selective oxidation of sulfides to sulfoxides.

ASSOCIATED CONTENT

Supporting Information

The Supporting Information is available free of charge at <https://pubs.acs.org/doi/10.1021/acs.inorgchem.0c02798>.

Table of bond lengths and angles, PXRD patterns, FT-IR spectra, TG curves, structural figures, and MS spectra (PDF)

Accession Codes

CCDC 2027080 and 2027081 contain the supplementary crystallographic data for this paper. These data can be obtained free of charge via www.ccdc.cam.ac.uk/data_request/cif, or by emailing data_request@ccdc.cam.ac.uk, or by contacting The Cambridge Crystallographic Data Centre, 12 Union Road, Cambridge CB2 1EZ, UK; fax: +44 1223 336033.

AUTHOR INFORMATION

Corresponding Authors

Xiang Wang — Liaoning Professional Technology Innovation Center of Liaoning Province for Conversion Materials of Solar

Cell, College of Chemistry and Materials Engineering, Bohai University, Jinzhou 121000, P. R. China; orcid.org/0000-0002-3793-6174; Email: xwang@bhu.edu.cn

Xiu-Li Wang – Liaoning Professional Technology Innovation Center of Liaoning Province for Conversion Materials of Solar Cell, College of Chemistry and Materials Engineering, Bohai University, Jinzhou 121000, P. R. China; orcid.org/0000-0002-0308-1403; Email: wangxiuli@bhu.edu.cn

Authors

Tong Zhang – Liaoning Professional Technology Innovation Center of Liaoning Province for Conversion Materials of Solar Cell, College of Chemistry and Materials Engineering, Bohai University, Jinzhou 121000, P. R. China

Yunhui Li – Liaoning Professional Technology Innovation Center of Liaoning Province for Conversion Materials of Solar Cell, College of Chemistry and Materials Engineering, Bohai University, Jinzhou 121000, P. R. China

Jiafeng Lin – Liaoning Professional Technology Innovation Center of Liaoning Province for Conversion Materials of Solar Cell, College of Chemistry and Materials Engineering, Bohai University, Jinzhou 121000, P. R. China

Huan Li – Liaoning Professional Technology Innovation Center of Liaoning Province for Conversion Materials of Solar Cell, College of Chemistry and Materials Engineering, Bohai University, Jinzhou 121000, P. R. China

Complete contact information is available at:

<https://pubs.acs.org/10.1021/acs.inorgchem.0c02798>

Notes

The authors declare no competing financial interest.

ACKNOWLEDGMENTS

The National Natural Science Foundation of China (Grants 21771025, 21971024, 21671025, and 21501013), General Program Fund for Education Department of Liaoning Province (LJ2019004), and Liao Ning Revitalization Talents Program (XLYC1902011) are gratefully acknowledged.

REFERENCES

- (1) Dolbecq, A.; Dumas, E.; Mayer, C. R.; Mialane, P. Hybrid Organic–Inorganic Polyoxometalate Compounds: From Structural Diversity to Applications. *Chem. Rev.* **2010**, *110*, 6009–6048.
- (2) Benseghir, Y.; Lemarchand, A.; Duguet, M.; Mialane, P.; Gomez-Mingot, M.; Roch-Marchal, C.; Pino, T.; Ha Thi, M. H.; Haouas, M.; Fontecave, M.; Dolbecq, A.; Sassoye, C.; Mellot-Draznieks, C. Co-immobilization of A Rh Catalyst and A Keggin Polyoxometalate in the UiO-67 Zr-Based Metal–Organic Framework: In Depth Structural Characterization and Photocatalytic Properties for CO₂ Reduction. *J. Am. Chem. Soc.* **2020**, *142*, 9428–9438.
- (3) Hou, Y.; Pang, H. J.; Zhang, L.; Li, B. N.; Xin, J. J.; Li, K.; Ma, H. Y.; Wang, X. M.; Tan, L. C. Highly Dispersive Bimetallic Sulfides Afforded by Crystalline Polyoxometalate-based Coordination Polymer Precursors for Efficient Hydrogen Evolution Reaction. *J. Power Sources* **2020**, *446*, 227319.
- (4) Singh, V.; Padhan, A. K.; Adhikary, S. D.; Tiwari, A.; Mandal, D.; Nagaiah, T. C. Poly(ionic liquid)–zinc Polyoxometalate Composite as A Binder-free Cathode for High-Performance Lithium–Sulfur Batteries. *J. Mater. Chem. A* **2019**, *7*, 3018–3023.
- (5) Wang, G. N.; Chen, T. T.; Gómez-García, C. J.; Zhang, F.; Zhang, M. Y.; Ma, H. Y.; Pang, H. J.; Wang, X. M.; Tan, L. C. A High-Capacity Negative Electrode for Asymmetric Supercapacitors Based on a PMo₁₂ Coordination Polymer with Novel Water-Assisted Proton Channels. *Small* **2020**, *16*, 2001626.
- (6) Cameron, J. M.; Wales, D. J.; Newton, G. N. Shining a Light on the Photo-sensitisation of Organic–inorganic Hybrid Polyoxometalates. *Dalton. Trans.* **2018**, *47*, 5120–5136.
- (7) Boulmier, A.; Vacher, A.; Zang, D.; Yang, S.; Saad, A.; Marrot, J.; Oms, O.; Mialane, P.; Ledoux, I.; Ruhlmann, L.; Lorcy, D.; Dolbecq, A. Anderson-Type Polyoxometalates Functionalized by Tetrathiafulvalene Groups: Synthesis, Electrochemical Studies, and NLO Properties. *Inorg. Chem.* **2018**, *57*, 3742–3752.
- (8) De Sousa, P. M. P.; Grazina, R.; Barbosa, A. D. S.; de Castro, B.; Moura, J. J. G.; Cunha-Silva, L.; Balula, S. S. Insights into the Electrochemical Behaviour of Composite Materials: Monovacant Polyoxometalates@Porous Metal–Organic Framework. *Electrochim. Acta* **2013**, *87*, 853–859.
- (9) Kanoo, P.; Ghosh, A. C.; Maji, T. K. A Vanadium (VO₂⁺) Metal–Organic Framework: Selective Vapor Adsorption, Magnetic Properties, and Use as A Precursor for A Polyoxovanadate. *Inorg. Chem.* **2011**, *50*, 5145–5152.
- (10) Li, J. K.; Huang, X. Q.; Yang, S.; Ma, H. W.; Chi, Y. N.; Hu, C. W. Four Alkoxohexavanadate-Based Pd-Polyoxovanadates as Robust Heterogeneous Catalysts for Oxidation of Benzyl-Alkanes. *Inorg. Chem.* **2015**, *54*, 1454–1461.
- (11) Linnenberg, O.; Mayerl, L.; Monakhov, K. Y. The Heck Reaction as a Tool to Expand Polyoxovanadates Towards Thiol-Sensitive Organic–inorganic Hybrid Fluorescent Switches. *Dalton. Trans.* **2018**, *47*, 14402–14407.
- (12) Stuckart, M.; Monakhov, K. Y. Vanadium: Polyoxometalate Chemistry. In *Encyclopedia of Inorganic and Bioinorganic Chemistry* Scott, R. A., Ed.; 2018; pp 1–19.
- (13) Monakhov, K. Y.; Bensch, W.; Kögerler, P. Semimetal-Functionalised Polyoxovanadates. *Chem. Soc. Rev.* **2015**, *44*, 8443–8483.
- (14) De Luis, R. F.; Orive, J.; Larrea, E. S.; Karmele Urtiaga, M.; Arriortua, M. I. Hybrid Vanadates Constructed from Extended Metal–Organic Arrays: Crystal Architectures and Properties. *CrystEngComm* **2014**, *16*, 10332–10366.
- (15) Wang, K.; Niu, Y. J.; Zhao, D. Y.; Zhao, Y. X.; Ma, P. T.; Zhang, D. D.; Wang, J. P.; Niu, J. Y. The Polyoxovanadate-Based Carboxylate Derivative K₆H[V^V₁₇V^{IV}₁₂(OH)₄O₆₀(OOC(CH₂)₄COO)₈].nH₂O: Synthesis, Crystal Structure, and Catalysis for Oxidation of Sulfides. *Inorg. Chem.* **2017**, *56*, 14053–14059.
- (16) Xu, N.; Gan, H. M.; Qin, C.; Wang, X. L.; Su, Z. M. From Octahedral to Icosahedral Metal–Organic Polyhedra Assembled from Two Types of Polyoxovanadate Clusters. *Angew. Chem., Int. Ed.* **2019**, *58*, 4649–4653.
- (17) Breen, J. M.; Clérac, R.; Zhang, L.; Cloonan, S. M.; Kennedy, E.; Feeney, M.; McCabe, T.; Williams, D. C.; Schmitt, W. Self-assembly of Hybrid Organic–Inorganic Polyoxovanadates: Functionalised Mixed-Valent Clusters and Molecular Cages. *Dalton. Trans.* **2012**, *41*, 2918–2926.
- (18) Zheng, L. M.; Wang, X. Q.; Wang, Y. S.; Jacobson, A. J. Syntheses and Characterization of Co₂(4,4′-bipy)₂(V₄O₁₂), Co(pz)-(VO₃)₂ and Co₂(2-pzc)(H₂O)(VO₃)₃ (4,4′-bipy = 4,4′-bipyridine, pz = pyrazine, 2-pzc = 2-pyrazinecarboxylate). *J. Mater. Chem.* **2001**, *11*, 1100–1105.
- (19) Chen, C. L.; Goforth, A. M.; Smith, M. D.; Su, C. Y.; Zur Loye, H.-C. [Co₂(ppca)₂(H₂O)(V₄O₁₂)_{0.5}]: A Framework Material Exhibiting Reversible Shrinkage and Expansion Through a Single-Crystal-to-Single-Crystal Transformation Involving a Change in the Cobalt Coordination Environment. *Angew. Chem., Int. Ed.* **2005**, *44*, 6673–6677.
- (20) Tian, H. R.; Zhang, Z.; Liu, S. M.; Dang, T. Y.; Li, X. H.; Lu, Y.; Liu, S. X. A Novel Polyoxovanadate-Based Co-MOF: Highly Efficient and Selective Oxidation of a Mustard Gas Simulant by Two-Site Synergetic Catalysis. *J. Mater. Chem. A* **2020**, *8*, 12398–12405.
- (21) Li, J. K.; Dong, J.; Wei, C. P.; Yang, S.; Chi, Y. N.; Xu, Y. Q.; Hu, C. W. Controllable Synthesis of Lindqvist Alkoxopolyoxovanadate Clusters as Heterogeneous Catalysts for Sulfoxidation of Sulfides. *Inorg. Chem.* **2017**, *56*, 5748–5756.

- (22) Lu, B. B.; Yang, J.; Liu, Y.-Y.; Ma, J. F. A Polyoxovanadate–Resorcin[4]arene-Based Porous Metal–Organic Framework as an Efficient Multifunctional Catalyst for the Cycloaddition of CO₂ with Epoxides and the Selective Oxidation of Sulfides. *Inorg. Chem.* **2017**, *56*, 11710–11720.
- (23) Cao, J. P.; Xue, Y. S.; Li, N. F.; Gong, J. J.; Kang, R. K.; Xu, Y. Lewis Acid Dominant Windmill-Shaped V₈ Clusters: A Bifunctional Heterogeneous Catalyst for CO₂ Cycloaddition and Oxidation of Sulfides. *J. Am. Chem. Soc.* **2019**, *141*, 19487–19497.
- (24) Wang, X. L.; Zhang, R.; Wang, X.; Lin, H. Y.; Liu, G. C. An Effective Strategy to Construct Novel Polyoxometalate-Based Hybrids by Deliberately Controlling Organic Ligand Transformation In Situ. *Inorg. Chem.* **2016**, *55*, 6384–6393.
- (25) Wang, X. L.; Zhang, R.; Wang, X.; Lin, H. Y.; Liu, G.-C.; Zhang, H. X. Three Novel and Various Isopolymolybdate-based Hybrids Built From the Carboxyl Oxygen Atoms of In Situ Ligands: Substituent-Tuned Assembly, Architectures and Properties. *Dalton Trans.* **2017**, *46*, 1965–1974.
- (26) Wang, X. L.; Zhang, R.; Wang, X.; Lin, H. Y.; Liu, G. C.; Zhang, H. X. Metal Ion-Tuned Coordination Polymers Based on Different Isopolymolybdates Grafted by In-Situ Ligand. *Polyhedron* **2017**, *135*, 180–188.
- (27) Aijaz, A.; Sañudo, E. C.; Bharadwaj, P. K. Construction of Coordination Polymers with a Bifurcating Ligand: Synthesis, Structure, Photoluminescence, and Magnetic Studies. *Cryst. Growth Des.* **2011**, *11*, 1122–1134.
- (28) Sheldrick, G. M. *SHELXS-2014, Program for Structure Solution*; University of Göttingen: Göttingen, Germany, 2014.
- (29) Sheldrick, G. M. *SHELXS-2014, Program for Structure Refinement*; University of Göttingen: Göttingen, Germany, 2014.
- (30) Li, S. B.; Sun, W. L.; Wang, K.; Ma, H. Y.; Pang, H. J.; Liu, H.; Zhang, J. X. Turn Helical Motifs from Pair to Single Entangled Double Helices in a Cobalt–Vanadate System via Introduction of a V-Shaped Ligand. *Inorg. Chem.* **2014**, *53*, 4541–4547.
- (31) Brown, I. D.; Altermatt, D. Bond-valence Parameters Obtained From a Systematic Analysis of the Inorganic Crystal Structure Database. *Acta Crystallogr., Sect. B: Struct. Sci.* **1985**, *41*, 244–247.
- (32) Paredes-García, V.; Gaune, S.; Saldías, M.; Garland, M. T.; Baggio, R.; Vega, A.; El Fallah, M. S.; Escuer, A.; Fur, E. L.; Venegas-Yazigi, D.; Spodine, E. Solvatomorphs of Dimeric Transition Metal Complexes Based on the V₄O₁₂ Cyclic Anion as Building Block: Crystalline Packing and Magnetic Properties. *Inorg. Chim. Acta* **2008**, *361*, 3681–3689.
- (33) Qi, Y. J.; Wang, Y. H.; Li, H. M.; Cao, M. H.; Hu, C. W.; Wang, E. B.; Hu, N. H.; Jia, H. Q. Hydrothermal Syntheses and Crystal Structures of Bimetallic Cluster Complexes [Cd(phen)₂]₂V₄O₁₂·5H₂O and [Ni(phen)₃]₂[V₄O₁₂]·17.5H₂O. *J. Mol. Struct.* **2003**, *650*, 123–129.
- (34) Zhang, Y.; Zapf, P. J.; Meyer, L. M.; Haushalter, R. C.; Zubieta, J. Polyoxoanion Coordination Chemistry: Synthesis and Characterization of the Heterometallic, Hexanuclear Clusters [Zn(bipy)₂]₂V₄O₁₂, [Zn(phen)₂]₂V₄O₁₂·H₂O, and [Ni(bipy)₂]₂Mo₄O₁₄. *Inorg. Chem.* **1997**, *36*, 2159–2165.
- (35) Fernández de Luis, R.; Urtiaga, M. K.; Mesa, J. L.; Larrea, E. S.; Iglesias, M.; Rojo, T.; Arriortua, M. I. Thermal Response, Catalytic Activity, and Color Change of the First Hybrid Vanadate Containing Bpe Guest Molecules. *Inorg. Chem.* **2013**, *52*, 2615–2626.
- (36) Devi, R. N.; Rabu, P.; Golub, V. O.; O'Connor, C. J.; Zubieta, J. Ligand Influences on the Structures of Copper(II) Vanadates. Structures and Magnetic Properties of [Cu₃(triazolate)₂V₄O₁₂], [Cu₂(tpyrpyz)₂V₄O₁₂] (tpyrpyz = tetrapyridylpyrazine) and [Cu₂(pyrazine)V₄O₁₂]. *Solid State Sci.* **2002**, *4*, 1095–1102.
- (37) Daniel, C.; Hartl, H. A Mixed-Valence V^{IV}/V^V Alkoxopolyoxovanadium Cluster Series [V₆O₈(OCH₃)₁₁]^{n±}: Exploring the Influence of a μ-Oxo Ligand in a Spin Frustrated Structure. *J. Am. Chem. Soc.* **2009**, *131*, S101–S114.
- (38) Zhu, Z.; Xu, C. G.; Wang, M.; Zhang, X.; Wang, H.; Luo, Q. D.; Bi, S. Y.; Fan, Y. H. Six Co(II) Coordination Polymers Based on Two Isomeric Semirigid Ether-Linked Aromatic Tetracarboxylate Acid: Syntheses, Structural Comparison, and Magnetic Properties. *Cryst. Growth Des.* **2017**, *17*, 5533–5543.
- (39) Li, D. S.; Zhao, J.; Wu, Y. P.; Liu, B.; Bai, L.; Zou, K.; Du, M. Co₅/Co₈-Cluster-Based Coordination Polymers Showing High-Connected Self-Penetrating Networks: Syntheses, Crystal Structures, and Magnetic Properties. *Inorg. Chem.* **2013**, *52*, 8091–8098.
- (40) Carreno, M. C. Applications of Sulfoxides to Asymmetric Synthesis of Biologically Active Compounds. *Chem. Rev.* **1995**, *95*, 1717–1760.
- (41) Fernández, I.; Khair, N. Recent Developments in the Synthesis and Utilization of Chiral Sulfoxides. *Chem. Rev.* **2003**, *103*, 3651–3706.
- (42) Dong, J.; Hu, J. F.; Chi, Y. N.; Lin, Z. G.; Zou, B.; Yang, S.; Hill, C. L.; Hu, C. W. A Polyoxoniobate–Polyoxovanadate Double-Anion Catalyst for Simultaneous Oxidative and Hydrolytic Decontamination of Chemical Warfare Agent Simulants. *Angew. Chem., Int. Ed.* **2017**, *56*, 4473–4477.
- (43) Li, J. K.; Huang, X. Q.; Yang, S.; Xu, Y. Q.; Hu, C. W. Controllable Synthesis, Characterization, and Catalytic Properties of Three Inorganic–Organic Hybrid Copper Vanadates in the Highly Selective Oxidation of Sulfides and Alcohols. *Cryst. Growth Des.* **2015**, *15*, 1907–1914.
- (44) Cao, J. P.; Xue, Y. S.; Li, N. F.; Gong, J. J.; Kang, R. K.; Xu, Y. Lewis Acid Dominant Windmill-Shaped V₈ Clusters: A Bifunctional Heterogeneous Catalyst for CO₂ Cycloaddition and Oxidation of Sulfides. *J. Am. Chem. Soc.* **2019**, *141*, 19487–19497.
- (45) An, H. Y.; Hou, Y. J.; Wang, L.; Zhang, Y. M.; Yang, W.; Chang, S. Z. Evans–Showell-Type Polyoxometalates Constructing High-Dimensional Inorganic–Organic Hybrid Compounds with Copper–Organic Coordination Complexes: Synthesis and Oxidation Catalysis. *Inorg. Chem.* **2017**, *56*, 11619–11632.
- (46) Kirillova, M. V.; Kuznetsov, M. L.; Romakh, V. B.; Shul'pina, L. S.; Fraústo da Silva, J. J. R.; Pombeiro, A. J. L.; Shul'pin, G. B. Mechanism of Oxidations with H₂O₂ Catalyzed by Vanadate Anion or Oxovanadium(V) Triethanolamine (vanadatrane) in Combination with Pyrazine-2-carboxylic acid (PCA): Kinetic and DFT Studies. *J. Catal.* **2009**, *267*, 140–157.
- (47) Smith, T. S.; Pecoraro, V. L. Oxidation of Organic Sulfides by Vanadium Haloperoxidase Model Complexes. *Inorg. Chem.* **2002**, *41*, 6754–6760.
- (48) Wang, X. S.; Huang, Y. B.; Lin, Z. J.; Cao, R. Phosphotungstic Acid Encapsulated in the Mesocages of Amine-functionalized Metal–organic Frameworks for Catalytic Oxidative Desulfurization. *Dalton Trans.* **2014**, *43*, 11950–11958.